A Novel Precoding and Impulsive Noise Mitigation Scheme for MIMO Power Line Communication Systems

Yuwen Qian, Xiangwei Zhou, Jun Li, Feng Shu, and Dushantha Nalin K. Jayakody, *Member, IEEE*

***Abstract*—Power line communications (PLCs) enable new and flexible networking functions in smart grids. However, due to the high attenuation and interference, it is a great challenge for PLC to achieve reliable and high data rate transmissions. Thus, we propose a multiple-input multiple-output (MIMO) architecture to improve the reliability and data rate for PLC networks. In viewing the data rate requirements of in-home PLC network systems, we develop a precoding scheme to maximize the system throughput. In harmonizing to the proposed precoding scheme, the closed-form of the sum data rate of the PLC-MIMO channel is derived. To improve the communication reliability, we propose a partial transmission sequence (PTS) based algorithm to mitigate the noise in PLC channels. The closed-form of the symbol error rate (SER) is derived according to the probability density function of the impulsive noise in PLC channels. Simulation results demonstrate that the proposed precoding scheme achieves a better throughput when compared to the conventional precoding schemes. Furthermore, the PTS-based noise mitigation algorithm significantly improves the SER performance of PLC links.**

***Index Terms*—Impulsive noise, multi-input multi-output, power line communications (PLCs), precoding, smart grid.**

Manuscript received February 13, 2017; revised May 23, 2018 and October 27, 2018; accepted November 4, 2018. Date of publication December 3, 2018; date of current version February 22, 2019. This work was supported in part by the National Natural Science Foundation of China under Grants 61727802, 61872184, 61801453, 61771244, 61702258, 61501238, 61472190, and 61271230, in part by the Jiangsu Provincial Science Foundation under Project BK20150786, in part by the Open Research Fund of National Key Laboratory of Electromagnetic Environment, China Research Institute of Radiowave Propagation under Grant 201500013, in part by the Specially Appointed Professor Program in Jiangsu Province 2015, in part by the Fundamental Research Funds for the Central Universities under Grant 30916011205, in part by the Open Research Fund of National Mobile Communications Research Laboratory, Southeast University, under Grants 2017D04 and 2013D02 and in part by the framework of the Competitiveness Enhancement Program of the National Research Tomsk Polytechnic University No. TPU CEP_IC_110\2017. *(Corresponding author: Jun Li.)*

Y. Qian and F. Shu are with the School of Electronic and Optical Engineering, Nanjing University of Science and Technology, Nanjing 210094, China (e-mail: admon@njust.edu.cn; shufeng0101@163.com).

X. Zhou is with the Division of Electrical and Computer Engineering, Louisiana State University, Baton Rouge, LA 70803 USA (e-mail: xwzhou@lsu.edu).

J. Li is with the School of Electronic and Optical Engineering, Nanjing University of Science and Technology, Nanjing 210094, China, with the National Mobile Communications Research Laboratory, Southeast University, Nanjing 210018, China, and also with the School of Computer Science and Robotics, National Research Tomsk Polytechnic University, Tomsk 634050, Russia (e-mail: jun.li@njust.edu.cn).

D. N. K. Jayakody is with the Department of Software Engineering, Institute of Cybernetics, National Research Tomsk Polytechnic University, Tomsk 634050, Russia (e-mail: nalin@tpu.ru).

Digital Object Identifier 10.1109/JSYST.2018.2880962

I. Introduction

THE power line communication (PLC) network is becoming a popular alternative for smart grids in extending the coverage of local area networks, such as access networks and in-home networks [1]. However, due to the high attenuation and interference natured in PLC channels, it will be a great challenge to improve the transmission performance [2]. Most PLC standards adopt multiple-input multiple-output (MIMO) techniques [3], in which more than two wires are utilized to carry information, thereby providing a higher data rate and better coverage [4]. Nevertheless, the performance bottlenecks of such MIMO systems are caused by self-interference due to MIMO transmissions and impulsive noises in PLC systems. An effective approach to mitigating self-interference is to adopt precoding schemes, which can increase data rate by implementing channel decoupling at the transmitters [5].

Precoding techniques in wireless networks have been extensively studied [6], [7]. Although the experience gained in wireless applications can be borrowed by PLC-MIMO systems for precoding design [8], channel characteristics of the power line and wireless media are basically different. In wireless channels, fading comes from time-varying constructive and destructive combinations of multiple path signals. The fading in PLC channels is caused by not only the signal reflections in the branch-based grid topology [9], which is like the signal reflections in wireless communications, but also the signal attenuations at each capacitor bank or transformer [10]. Furthermore, the noise in the wireless channel is assumed to be dominated by the thermal one. On the contrary, the noise in the PLC channel is modeled as the colored background and asynchronous impulsive noises. Therefore, many mature precoding algorithms in wireless MIMO networks, designed based on the features of wireless channels, no longer work effectively in PLC networks [11].

Recent studies focus on precoding schemes in MIMO-based PLC systems for performance enhancement [5], [12]. In these studies, iterative algorithms are usually adopted to obtain a suboptimal solution. However, the computational complexities of these precoding methods are still high. Hence, designing efficient precoding schemes with a low-complexity for MIMO-based PLC networks is a challenging problem. At the same time, as orthogonal frequency division multiplexing (OFDM) has been utilized in PLC-MIMO systems for strengthening the spectrum efficiency, proper precoding design can improve

the transmission performance by effectively mitigating the self-interference [13]. Nevertheless, impulsive noises in PLC systems can hardly be removed, causing a performance deterioration [14]. How to reduce impulsive noises is another challenge in PLC systems [15].

In concord with the work presented in [16], the impulsive noises affect the PLC system severely when its power exceeds a certain threshold. An effective method for reducing the adverse effect caused by impulsive noise, namely, a blanking approach, is proposed in [17]. This strategy involves receiving one signal whose power is larger than the selected threshold, which will be set as null. Based on this idea, a nonlinear preprocessor with blanking, clipping, or hybrid has been proposed in [18]. Since this approach is very simple to implement for improving the system performance, it has been widely used in practical OFDM-based PLC systems. Nonetheless, these methods mitigate the impulsive based on the accurate prior knowledge of the noise. As referred in [19], small error estimations of the IN can cause the significant performance degradation. In this case, Alsusa and Rabie [19] have proposed to blank the impulsive noise with the optimal blanking threshold (OBT) by estimating the signals' peak-to-average-power ratio (PAPR). Based on this, [20] implement the OBT estimation and design the impulsive noise blanking algorithm with dynamic peak-based threshold estimation (DPTE). Compared to the impulsive noise blanking algorithm without estimating the OBT, the DPTE-based impulsive noise blanking algorithm can improve the gain of up to 2.5 dB. Furthermore, DPTE-based impulsive noise blanking algorithm need the prior knowledge about the characteristics of impulsive noise.

In addition, due to the high PAPR of the OFDM signals, the received power of useful signals are often larger than the selected threshold. Therefore, the high PAPR can lead to the imperfect recognition of the impulsive signal, and thus the useful signals are blanked and clipped or some impulsive noise signals are overlooked. This leads to a dramatic performance degradation. To solve the problem, the effective approach is to apply the well-known PAPR reduction scheme. The partial transmission sequence (PTS) is known as the effective approach to compress PAPR[21], and PTS-based impulsive noise mitigation (INM) approach can improve the symbol error rate (SER) performance. In the work presented in [22], Rabie and Alsusa have proposed the DPTE-PTS algorithm to improve the performance according to the blanking error probability, probability of missed blanking, and probability of successful detection. Moreover, Rabie and Alsusa [23] analyzed the performance of the system with the DPTE-PTS algorithm by deriving the closed-form for the SER and output signal-to-noise ratio (SNR). As in [18], the performance is analyzed based on the assumption that signals are transmitted over a Rayleigh channel. However, these techniques require side information transmission, which can be energy consuming and challenging to implement in practice for PLC channels with non-Gaussian noise. To tackle this issue, vector OFDM (VOFDM), which has inherently good PAPR features, has been proposed in [24] for the PLC system and nulling and clipping are implemented at the receiver to further improve the performance. From the numerical results, the VOFDM scheme can provide up to 2 dB transmit power savings compared to the conventional OFDM to meet the same performance requirement. Generally, the performance analysis in these works is based on the fact that the fading of PLC channels follows the Rayleigh distribution. However, it is more practical that the fading of PLC channels follows the lognormal distribution. The analysis for the PLC channel with the lognormal fading in the impulsive mitigation system is the challenge.

In this paper, we propose the precoding and impulsive mitigating scheme for the PLC-MIMO systems, which is effective in increasing the data rate by mitigating self-interference. In particular, we list out our fourfold contributions as follows.

1) The PLC-MIMO system with impulsive noise is modeled as a Markov process. Considering that the noise varies with the state of the Markov process, we design the precoding scheme for the PLC-MIMO system in each system state. The transmitter can adaptively select the precoder for the system states by perceiving channel state information (CSI).
2) By solving the optimal problem of maximizing the sum rate, we design the precoder matrix for each transmitter. The closed-form expression is derived for the sum rate of the PLC-MIMO channel based on the designed precoder matrix.
3) By modeling the PLC channel as the VOFDM system, we propose a hybrid noise mitigation algorithm of the blanking [17] and clipping [18] to mitigate the impulsive noise. To protect useful signals from being removed, the PTS is used to reduce the PAPR of transmitting signals.
4) We derive the closed-form of the output SNR for the PLC channel through hybrid noise mitigation of algorithm. To the authors' best knowledge, this is the first attempt to analyze the performance of the INM algorithm where the channel fading follows the lognormal distribution.

The remainder of this paper is organized as follows. Section II describes the PLC-MIMO system based on OFDM. Section III formulates the precoding problem in PLC-MIMO systems to maximize the sum data rates, and a closed-form of the sum data rates is derived. Section IV presents the hybrid noise mitigation algorithm based on PTS. Section V provides numerical results to demonstrate the performance of the proposed algorithms. Finally, Section VI concludes the paper.

II. PLC-MIMO Channel Model

The PLC-MIMO system is constructed with the combination of the power line structure shown in Fig. 1 and the typical MIMO model. The three-wire power line is composed of a phase ($\mathcal{P}$), a neutral ($\mathcal{N}$), and a protective earth ($\mathcal{PE}$) [25]. Signals are transmitted as the voltage difference between two power wires, and thus there are three kinds of transmission (or input) ports, i.e., $\mathcal{P}$ to $\mathcal{N}$, $\mathcal{P}$ to $\mathcal{PE}$, and $\mathcal{N}$ to $\mathcal{PE}$. In the system, two ports are exploited as the communication sockets for the reason that the sum of the voltage difference between the three lines is zero, according to Kirchhoff's law in the circuit.

We adopt OFDM to improve spectrum efficiency in our PLC-MIMO system, and employ the adaptive modulation to modulate

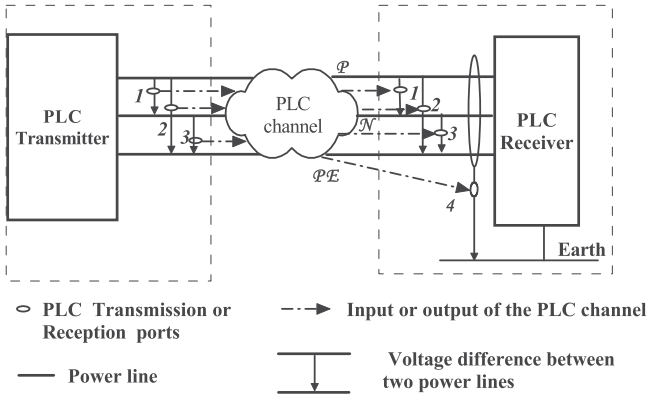

Fig. 1. PLC channel for a three-wire installation, where signals are transmitted with pairs of wires. There are three transmission (or input) ports: $\mathcal{N}-\mathcal{PE}$, $\mathcal{P}-\mathcal{N}$, and $\mathcal{P}-\mathcal{PE}$, and four reception (or output) ports $\mathcal{N}-\mathcal{PE}$, $\mathcal{P}-\mathcal{N}$, $\mathcal{P}-\mathcal{PE}$, and sum$(\mathcal{P},\mathcal{PE},\mathcal{N})$-earth.

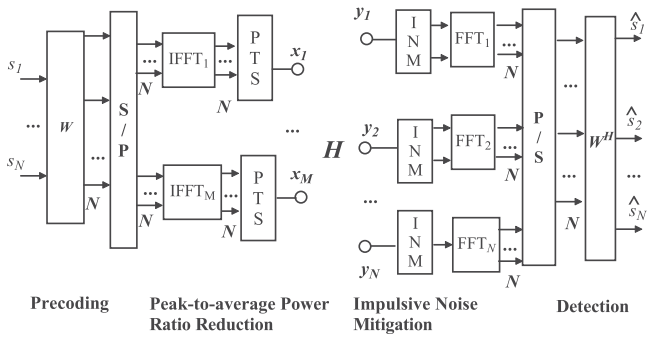

Fig. 2. OFDM scheme with M transmission ports and N reception ports in the PLC-MIMO channel $\mathbf{H}$, where the PTS module is installed to reduce the peak-to-average power ratios of the signals, s_n $(n=1,\ldots,N)$ is the input QAM symbol, W is the precoding matrix, x_m $(m=1,\ldots,M)$ is the transmitted signal from mth transmission ports, y_n $(n=1,\ldots,N)$ is the received signal by nth reception ports, and $\widehat{s}_n$ $(n=1,\ldots,N)$ is the output symbol.

input signals. When receiving the OFDM signal, the receiver utilizes an INM component to mitigate the impulsive noise in the PLC channel. Fig. 2 illustrates our system.

Generally, the PLC-MIMO channel with M transmission ports and N reception ports has the channel matrix $\mathbf{H}$, described by

$$\mathbf{H}=\begin{bmatrix} h_{1,1} & \cdots & h_{1,m} & \cdots & h_{1,M} \\ \vdots & \ddots & \vdots & \ddots & \vdots \\ h_{n,1} & \cdots & h_{n,m} & \cdots & h_{2,M} \\ \vdots & \ddots & \vdots & \ddots & \vdots \\ h_{N,1} & \cdots & h_{N,m} & \cdots & h_{N,M} \end{bmatrix} \tag{1}$$

where $h_{n,m}(m=1,\ldots,M$ and $n=1,\ldots,N)$ is the complex channel transfer function coefficient from the mth transmission port to the nth reception port. As in [26], the time domain expression of $h_{n,m}$ can be given by

$$h_{n,m}=\sum_{i=1}^{L_{m,n}} g_{m,n,i}A_{m,n}(f,\ell_{m,n,i})e^{-j2\pi f\tau_{m,n,i}} \tag{2}$$

where $L_{m,n}$ is the number of the propagation paths from the mth transmission port to the nth reception port, f is the natural frequency, $\ell_{m,n,i}$ is the power line length from the mth transmission port to the nth reception port over the ith propagation path, $\tau_{m,n,i}$ is the delay related with $\ell_{m,n,i}$, $g_{m,n,i}$ is the weighting factor comprised of the reflection and transmission factors along the propagation path, and $A_{m,n}(f,\ell_{m,n,i})$ is the attenuation that increases with the frequency f. Furthermore, by assuming that signals are transmitted at the same speed over each path, we can approximate $A_{m,n}(f,\ell_{m,n,i})$ as

$$A_{m,n}\left(f,\ell_{m,n,i}\right)=e^{-(a_0+a_1\cdot f^q)\cdot\ell_{m,n,i}} \tag{3}$$

where the constants a_0, a_1, and q can be obtained by measuring the frequency response of PLC systems.

Especially, we consider the PLC systems shown in Fig. 2 as the 2×2 MIMO PLC system, where there are two transmitters and two receivers. Accordingly, the channel matrix $\mathbf{H}$ is

$$\mathbf{H}=\begin{pmatrix} h_{1,1} & h_{1,2} \\ h_{2,1} & h_{2,2} \end{pmatrix}. \tag{4}$$

For the nth $(1\le n\le N)$ reception port, the received signal y_n can be expressed as

$$y_n=\sum_{m=1}^{M} h_{n,m}x_m+z_n \tag{5}$$

where x_m is the signal transmitted from the mth transmission port, and z_n is the received noise at the nth reception port.

According to (1) and (5), we can describe the PLC-MIMO channel model as

$$\mathbf{y}=\mathbf{H}\mathbf{x}+\mathbf{z} \tag{6}$$

where $\mathbf{x}=[x_1,x_2,\ldots,x_M]^T$ is the transmitting signal vector, $\mathbf{y}=[y_1,y_2,\ldots,y_N]^T$ is the receiving signal vector, and $\mathbf{z}=[z_1,z_2,\ldots,z_N]^T$ is the noise vector.

In the following, we take a series of steps to describe the noise $\mathbf{z}$ in (6), which is generally known as a combination of Gaussian and impulsive noises.

First, consorting to the work presented in [27], we model the impulsive noise as a non-redundant and periodic stable Markov process with an infinite number of states. Thus, the state set is

$$\mathbf{u}=[\mu_0,\ldots,\mu_\eta,\ldots,\mu_\Theta]^T,0\le\eta\le\Theta \tag{7}$$

where $\Theta(\Theta\to\infty)$ is the total state number.

By resorting to the memoryless nature of the system, we define

$$p_{kj}=\Pr\left(S_{l+1}=\mu_k|S_l=\mu_j\right) \tag{8}$$

where S_l represents the state of the system at time l, and p_{kj} is the state transfer probability of the event that the system is at the jth $(1\le j\le\Theta)$ state at time l and shifts to the kth $(1\le k\le\Theta)$ state at time $l+1$.

Second, as given in [27], the state probability in the Markov process is given by

$$\Pr(\mu_\eta=m)=e^{-G}\frac{G^m}{m!},m\ge 0 \tag{9}$$

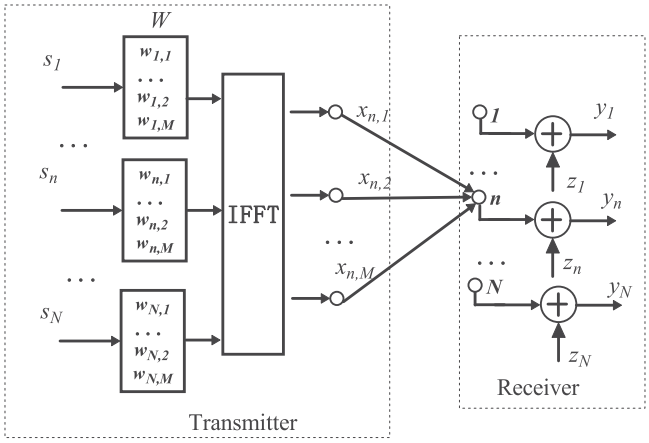

Fig. 3. Precoding scheme of the PLC system, $x_{n,1}, x_{n,2}, \ldots, x_{n,M}$ are signals emitted by the M transmission ports to the nth reception port, $y_n\,(n = 1, \cdots N)$ is the received signal of the nth reception ports, and $z_n\,(n = 1, \ldots, N)$ is the received noises from the nth ports.

where G is the impulsive index that depends on the average number of impulses per unit time.

With the statistical method presented in [10] and (9), the probability density function (PDF) of the amplitude of the impulsive noise is given by

$$f(x) = e^{-G} \sum_{\eta=0}^{\infty} \frac{G^{\eta}}{\eta! \sqrt{2\pi\sigma_{\eta}^2}} e^{-\frac{x^2}{2\sigma_{\eta}^2}} \tag{10}$$

where $\sigma_{\eta}^2 = \sigma^2 \cdot \frac{(\eta/G+\Gamma)}{(1+\Gamma)}$, $\sigma^2 = \sigma_g^2 + \sigma_i^2$, $\Gamma = \sigma_g^2/\sigma_i^2$, σ^2 is the total noise power that equals the sum of impulsive and Gaussian noise powers, σ_i^2 is the impulsive noise power, σ_g^2 is the Gaussian noise power, and Γ denotes the power ratio between the Gaussian noise and impulsive noise.

As originally given in [28], the combination of the Gaussian and impulsive noises can be modeled as a Bernoulli Gaussian random process

$$z = z_g + z_i \tag{11}$$

where z_g is the Gaussian noise, and z_i is the impulsive noise.

III. Precoding Algorithm

In this section, we design a precoding scheme for the PLC-MIMO system, as shown in Fig. 3.

As given in (10), the power of the noise in the ηth state can be given as

$$\sigma_{\eta}^2 = \sigma^2 \left(\frac{\frac{\eta}{G} + \Gamma}{1 + \Gamma} \right). \tag{12}$$

From (12), we notice that the noise of the system in the ηth state is different from that of the system in the $(\eta + 1)$th state. Since the data rate is dominated by the noise and transmit power, the data rate in each state is different from each other as the transmit power is assumed to be fixed. Furthermore, according to the work presented in [29], the noise of each state can be taken as a Gaussian noise. In this case, we present our precoding algorithm to maximize the sum data rate for each system state.

We select the ηth $(1 \leq \eta \leq \Theta)$ state to design the precoding matrix. Let us denote s_n as the signal sent to the nth $(1 \leq n \leq N)$ reception port. In the following, we take the procedure of transmitting s_n in the PLC-MIMO system as an example to derive the precoding matrix for the ηth state.

As s_n is transmitted in the ηth state, the transmitting signal vector $\mathbf{x}_n^{(\eta)} = [x_{n,1}, x_{n,2}, \ldots, x_{n,M}]$ from M transmission ports to the nth reception port is given by

$$\mathbf{x}_n^{(\eta)} = \mathcal{F}\mathbf{w}_n^{(\eta)} s_n \tag{13}$$

where $\mathcal{F}$ is the inverse fast Fourier transform (IFFT) transform matrix, $\mathbf{w}_n^{(\eta)} = [w_{n,1}^{(\eta)}, w_{n,2}^{(\eta)}, \ldots, w_{n,M}^{(\eta)}]^T$ is the precoding vector designed to send information for the nth receiving port in the ηth state, and $\mathbf{w}_n^{(\eta)^H} \mathbf{w}_n^{(\eta)} = 1$. Note that the power of the transmit ports are assumed to be normalized.

In the OFDM scheme, we use an equivalent frequency response $\widehat{h}_{n,m}$ for the PLC channels, given by

$$\widehat{h}_{n,m} = h_{n,m}\mathcal{F}. \tag{14}$$

According to (13) and (14), the received signal at the nth port is expressed as

$$y_n^{(\eta)} = \widehat{\mathbf{h}}_n \mathbf{w}_n^{(\eta)} s_n + \widehat{\mathbf{h}}_n \sum_{j=1, j\neq n}^{N} \mathbf{w}_j^{(\eta)} s_j + z_n^{(\eta)} \tag{15}$$

where $\widehat{\mathbf{h}}_n = [\widehat{h}_{n,1}, \widehat{h}_{n,2}, \ldots, \widehat{h}_{n,M}]$ is the channel vector of the nth receiving port, $z_n^{(\eta)}$ is the channel noise of the nth port with the variance $(\sigma_n^{(\eta)})^2$, s_j is the signal sent to the jth $(j = 1, \ldots, N$, and $j \neq n)$ receiving ports, and $\mathbf{w}_j^{(\eta)}$ is the precoding vector designed to send information for the jth receiving port.

Accordingly, s_j is the information sent to the jth port that can be also received by the nth port, which then introduces the self-interference to the nth port to receive information. Therefore, in our precoding algorithm, we need to mitigate these interferences to achieve higher data rate.

In the process of designing the precoding matrix of the nth receiving port in the ηth state, we first define two matrices $\mathbf{A}_{t,n}^{(\eta)}$ and $\mathbf{B}_{t,n}^{(\eta)}$, where $t(1 \leq t \leq N)$ is an integer. According to the relation between t and n, we give the definitions of $\mathbf{A}_{t,n}^{(\eta)}$ and $\mathbf{B}_{t,n}^{(\eta)}$ in two cases. In the first case, if $n = t$, we define $\mathbf{A}_{t,n}^{(\eta)}$ as

$$\mathbf{A}_{t,n}^{(\eta)} \triangleq \left(\left(\sigma_t^{(\eta)}\right)^2 + \sum_{t=1, t\neq n}^{N} \mathbf{w}_t^{(\eta)^H} \widehat{\mathbf{h}}_t^H \widehat{\mathbf{h}}_t \mathbf{w}_t^{(\eta)} \right) \mathbf{I}_{M\times M} \tag{16}$$

and $\mathbf{B}_{t,n}^{(\eta)}$ as

$$\mathbf{B}_{t,n}^{(\eta)} \triangleq \widehat{\mathbf{h}}_t^H \widehat{\mathbf{h}}_t + \mathbf{A}_{t,n}^{(\eta)}. \tag{17}$$

In the second case, if $n \neq t$, $\mathbf{A}_{t,n}$ is defined by

$$\mathbf{A}_{t,n}^{(\eta)} \triangleq \left(\left(\sigma_t^{(\eta)}\right)^2 + \sum_{j=1, j\neq n, j\neq t}^{N} \mathbf{w}_j^{(\eta)^H} \widehat{\mathbf{h}}_t^H \widehat{\mathbf{h}}_t \mathbf{w}_j^{(\eta)} \right) \cdot \mathbf{I}_{M\times M} + \widehat{\mathbf{h}}_{\mathbf{n}}^{\mathbf{H}} \widehat{\mathbf{h}}_{\mathbf{n}} \tag{18}$$

and $\mathbf{B}_{t,n}^{(\eta)}$ is defined by

$$\mathbf{B}_{t,n}^{(\eta)} \triangleq \mathbf{w}_t^{(\eta)^H} \widehat{\mathbf{h}}_t^H \widehat{\mathbf{h}}_t \mathbf{w}_t^{(\eta)} + \mathbf{A}_{t,n}^{(\eta)}. \tag{19}$$

Since $\mathbf{w}_n^{(\eta)^H} \mathbf{w}_n^{(\eta)} = 1$, $\mathbf{A}_{t,n}^{(\eta)}$ and $\mathbf{B}_{t,n}^{(\eta)}$ are semi-positive matrices. Then, we can calculate the achievable sum data rate of the N ports in the ηth state with Theorem 1.

Theorem 1: In PLC-MIMO systems with N reception ports under impulsive and Gaussian noises in the ηth $(1 \leq \eta \leq \Theta)$ state, as the signals precoded with $\mathbf{w}_n^{(\eta)}$ are transmitted to the nth $(1 \leq n \leq N)$ port, the achievable sum data rate of the N reception ports is given as

$$R_{\text{sum}}^{(\eta)}(n) = \log_2 \left(\prod_{t=1}^{N} \frac{\mathbf{w}_n^{(\eta)^H} \mathbf{B}_{t,n}^{(\eta)} \mathbf{w}_n^{(\eta)}}{\mathbf{w}_n^{(\eta)^H} \mathbf{A}_{t,n}^{(\eta)} \mathbf{w}_n^{(\eta)}} \right). \tag{20}$$

Proof: See Appendix A.

To calculate the maximal $R_{\text{sum}}^{(\eta)}(n)$ in (20), we define

$$\lambda\left(\mathbf{w}_n^{(\eta)}\right) = \prod_{t=1}^{N} \frac{\mathbf{w}_n^{(\eta)^H} \mathbf{B}_{t,n}^{(\eta)} \mathbf{w}_n^{(\eta)}}{\mathbf{w}_n^{(\eta)^H} \mathbf{A}_{t,n}^{(\eta)} \mathbf{w}_n^{(\eta)}}. \tag{21}$$

According to (20) and (21), computation of the maximal $R_{\text{sum}}^{(\eta)}$ is equivalent to computing the maximal $\lambda(\mathbf{w}_n^{(\eta)})$. By using Lagrange multipliers, we can obtain

$$\lambda\left(\mathbf{w}_n^{(\eta)}\right) = \left\{ \lambda\left(\mathbf{w}_n^{(\eta)}\right) \mid \det\left(\mathbf{V}\left(\mathbf{w}_n^{(\eta)}\right) - \lambda\left(\mathbf{w}_n^{(\eta)}\right) \mathbf{Q}\left(\mathbf{w}_n^{(\eta)}\right) = 0\right) \right\} \tag{22}$$

where

$$V\left(\mathbf{w}_n^{(\eta)}\right) = \sum_{j=1}^{N} \prod_{t=1, t\neq n}^{N} \mathbf{w}_n^{(\eta)^H} \mathbf{B}_{j,n}^{(\eta)} \mathbf{w}_n^{(\eta)} \mathbf{B}_{t,n}^{(\eta)} \tag{23}$$

and

$$Q\left(\mathbf{w}_n^{(\eta)}\right) = \sum_{j=1}^{N} \prod_{t=1, t\neq j}^{N} \mathbf{w}_n^{(\eta)^H} \mathbf{A}_{j,n}^{(\eta)} \mathbf{w}_n^{(\eta)} \mathbf{A}_{t,n}^{(\eta)}. \tag{24}$$

Since (22) is not convex, we cannot obtain the closed-form solution for $\mathbf{w}_n^{(\eta)}$. However, we can follow the generalized power iterative (GPI) algorithm proposed in [30] to obtain the approximate global solution for $\mathbf{w}_n^{(\eta)}$. By repeating GPI for N times, we can develop $W^{(\eta)}$ that is the precoding matrix used for the η state. Since, according to the work presented in [30], GPI is convergent, our approach to computing $W^{(\eta)}$ is also convergent with complexity $O(NI)$, where I is the complexity of the algorithm GPI.

It is assumed in this paper that the CSI is available at terminal nodes and the PLC channel is quasi-stationary (or quasi-cyclostationary) [31]. Thus, we use a feedback channel to obtain CSI, which can indicate the Markov state η for the PLC-MIMO system. In this way, the transmitter can select $W^{(\eta)}$ dynamically in terms of the dynamically obtained CSI. Since $W^{(\eta)}$ can be designed when initializing the system, we do not need to calculate $W^{(\eta)}$ for each time when the system state varies. As a result, the proposed precoding scheme works efficiently.

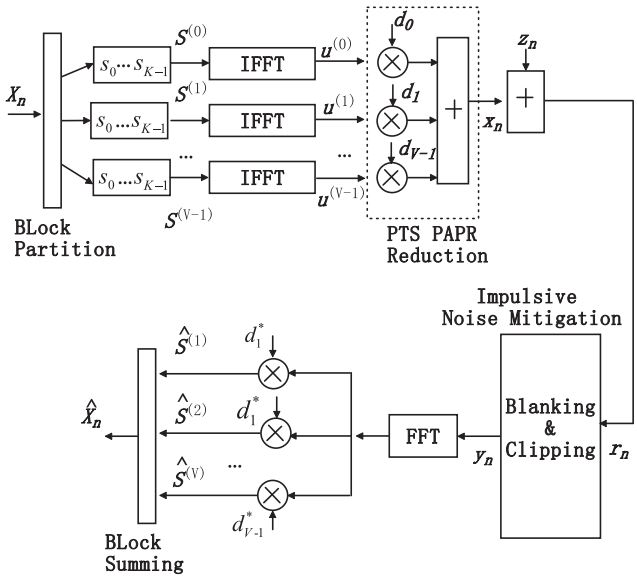

Fig. 4. PTS-based INM model, where X_n is the input 16-QAM symbol transmitted to the nth port, $u^{(v)}(v = 0, \ldots, V-1)$ is the signal in time domain after the IFFT transformation, $d_v(v = 0, \ldots, V-1)$ is the constructed complex phase factor used to reduce the PAPR, and r_n is the received signal from the nth port, y_n is the output signal of the INM, and $\hat{X}_n$ is the output of the INM system.

In addition, as we transmit signals to the nth port, the maximal sum data rate of the PLC-MIMO system with the proposed precoding algorithm in Θ states can be obtained as

$$R_{\text{sum}}(n) = \sum_{\eta=0}^{\Theta-1} \frac{e^{-G} G^{\eta}}{\eta!} R_{\text{sum}}^{(\eta)}(n). \tag{25}$$

IV. Impulsive Noise Mitigation

In this section, we present an INM approach according to the system states. We consider the channel between the mth transmission port and the nth reception ports in PLC-MIMO system. The PLC channel is modeled as a VOFDM system according to the work presented in [24]. The input signals are mapped into 16-quadratic-amplitude modulation (QAM) symbols, which then pass through an OFDM modulator. The time domain signal $u(\tau)$ produced by the OFDM modulator can be written as

$$u(\tau) = \frac{1}{\sqrt{K}} \sum_{k=0}^{K-1} s_k e^{\frac{j 2\pi k \tau}{T_s}}, \ 0 < \tau < T_p \tag{26}$$

where K is the number of sub-carriers, s_k is the input QAM symbols, T_s is the active symbol interval, and T_p is the period.

The PTS-based INM model is shown in Fig. 4. In the PTS algorithm, the transmitting information bits need to be partitioned into vectors. The information transmitted to the nth port $\mathbf{X_n}$ is first partitioned into V disjoint sub-blocks

$\mathbf{X}_n = [\mathbf{S}_n^{(0)}, \mathbf{S}_n^{(1)}, \ldots, \mathbf{S}_n^{(V)}]$. Since the sub-carrier number of the OFDM scheme is K, the vector $\mathbf{S}_n^{(v)}$ can be expressed as $[S_1^{(v)}, S_2^{(v)}, \ldots, S_K^{(v)}], v = 1, 2, \ldots V$.

A. PAPR Reduction

In this section, we use a PAPR reduction to reduce the PAPR of signals. The PAPR of signals is defined by

$$\Upsilon = \frac{\max |u(\tau)|^2}{\mathbb{E}\left(|u(\tau)|^2\right)} \tag{27}$$

where $\mathbb{E}(\cdot)$ is the statistical expectation.

Now, we use PTS-based approach to reduce PAPR. First, we transform the time domain signals $u^{(0)}, u^{(1)}, \ldots, u^{(V-1)}$ into frequency domain signals $u^{(0)}(f), u^{(1)}(f), \ldots, \ldots, u^{(K-1)}(f)$. Then, each frequency domain signal is multiplied by a corresponding complex phase factor, expressed as

$$x_n(f) = \sum_{v=0}^{V-1} d_v \cdot \mathcal{F}\left(S_n^{(v)}\right) = \sum_{v=0}^{V-1} d_n u^{(v)}(f) \tag{28}$$

where $x(f)$ is the frequency domain signal transmitted by the transmitting ports, and d_v is the complex phase factor, constructed by

$$d_v = e^{j\phi i}, \;\; i = 1, 2, \ldots, C \tag{29}$$

where C is a constant, and ϕ is the phase angle.

In the next step, we select the optimal phase factor vector $[d_0, \ldots, d_{V-1}]$ to satisfy

$$[d_0, \ldots, d_{V-1}] = \underset{[d_0, \ldots, d_{V-1}]}{\arg\min} \left(\max \left| \sum_{v=0}^{V-1} d_v u^{(v)}(f) \right| \right). \tag{30}$$

At last, we obtain the transmitted time domain signal, given by

$$x_n = \sum_{v=0}^{V-1} \left(d_v \otimes u^{(v)} \right) \tag{31}$$

where $\otimes$ represents the convolution.

Since the complexity of the approach depends on C, we utilize the binary-phase-factor algorithm presented in [32], where $C = 2$, to seek the optimal value for d_k to minimize PAPR of the input signal.

B. Noise Mitigation Scheme

In this section, we design a hybrid noise mitigation processor (HNMP) to mitigate noise in the PLC channel. The HNMP is a combination of the blanking [18] and clipping [33] noise mitigation. According to the work presented in [17], the blanking-based noise mitigation is the simplest and most effective method to make the impulsive noise null. The clipping-based method, however, is used to mitigate the noise created by the uncorrelated distort component, caused by the nonlinearity output of the Gaussian process.

To implement the HNMP, we need to select two amplitude thresholds, the clipping threshold T and blanking threshold aT. Generally, a is a constant larger than one. In this case, we can use three events to describe the receiving signals. The first event, denoted by D_0, represents that the amplitude of received signal is between 0 and T. If D_0 occurs, the received signals are taken as those transmitting signals without influenced by noises. Thus, we do not need to change them. Second, we use the event D_1 to indicate the received signal amplitudes between T and aT. As D_1 occurs, we clip the receiving signals. In the processing of clipping noise, the signal with maximal amplitude v_k is selected from the input signals of the HNMP $v_0, \ldots, v_{K-1}$, expressed as $\arg(v_k)$. Then, we use $Te^{j\arg(v_k)}$ as the output clipped signal. At last, the event D_2 implies that the received signal amplitudes are larger than aT. When D_2 occurs, the receiving signal is considered as the impulsive noise. Thus, we set its amplitude as zero.

As a result, the output signal $\tilde{v}_k$ of the HNMP can be expressed as

$$y_n = \begin{cases} r_n, & r_n \le T \\ Te^{j\arg(r_n)}, & T < |r_n| \le aT \\ 0, & |r_n| > aT \end{cases} \tag{32}$$

where v_k is the input signal of the HNMP.

According to (32), the output signal x_n can also be expressed as

$$y_n = \mathcal{K} \cdot h_{n,m} x_n + z_n \tag{33}$$

where $\mathcal{K}$ is a scaling factor, and z_n is the noise. Since z_n is independent with sending signals, $\mathbb{E}[z_n x_n^*] = 0$, where x_n^* is the conjugate signal of x_n.

$\mathcal{K}$ in (33) is given by the work presented in [34] as

$$\mathcal{K} = \frac{\mathbb{E}\left(y_n x_n^*\right)}{h_{n,m}^2 \mathbb{E}\left(|x_n|^2\right)} = \frac{1}{2h_{n,m}^2} \mathbb{E}\left(y_n x_n^*\right). \tag{34}$$

According to (32) and (33), we present the closed-form expression for the output SNR of the HNMP with Theorem 2.

Theorem 2: Given a PLC-OFDM channel subject to the combination of the impulsive and Gaussian noises, the output SNR γ for the HNMP can be given by

$$\gamma = \left(\frac{P_{\text{out}}}{2h_{n,m}^2 \mathcal{K}^2} - 1 \right)^{-1} \tag{35}$$

where P_{out} and $\mathcal{K}$ are the output signal power of the HNMP and the scaling factor, which are given by (36) and (37), respectively, in the following page.

$$P_{\text{out}} = \sum_{\eta=1}^{\Theta} {p_\eta}^2 Q_r(T) C_r Q_r \left(Te^{-2\pi\sigma_\eta^2} \right) + \sum_{\eta=1}^{\Theta} {p_\eta}^2 \left(Q_r\left(aT\right) - Q_r(T) \right) C_r \left(Q_r\left(aTe^{-2\pi\sigma_\eta^2} \right) - Q_r\left(Te^{-2\pi\sigma_\eta^2} \right) \right). \tag{36}$$

TABLE I
SIMULATION PARAMETERS SETTING

Parameter name	Value
Path parameter g_i	-0.15
Path number	5
Fading parameter a_0	0
Fading parameter a_1	7.8×10^{-10}
Impulsive noise power	-15dB
Probability of impulse occurrence p	0.01
Impulsive index A	0.1
Gaussian noise power	2.5dB

$$\mathcal{K} = \frac{1}{4}\sum_{\eta=1}^{\Theta}\left({p_\eta}^2 Q_r(T) C_r Q_r\left(Te^{-2\pi\sigma_\eta^2}\right) - \sum_{\varsigma\in\{s,z\}} \times \left(\sum_{i=1}^{N} H_i Q_\varsigma\left(T-\sigma_{g_\eta}^2-\xi_i\right) C_\varsigma Q_\varsigma\left(Te^{-2\pi\sigma_\varsigma^2}\right)\right)\right) + \frac{T}{4}\sum_{\eta=1}^{\Theta} {p_\eta}^2 \left(Q_r(aT) - Q_r(T)\right) \times \left(\sum_{\chi\in\{r,Z_1,Z_2\}} \widetilde{C}_\chi\left(Q_\chi\left(aTe^{-\pi\sigma_\chi^2}\right) - Q_{Z_2}\left(Te^{-\pi\sigma_\chi^2}\right)\right)\right). \quad (37)$$

In (36) and (37), $Q_i(\cdot)$ is

$$Q_i(x) = \int_{-\infty}^{\frac{\ln(x)-\mu_i}{\sqrt{2\pi\sigma_i^2}}} e^{-t^2}\,dt, \quad i \in \{r, s, z, Z_1, Z_1\}. \quad (38)$$

In addition, C_j and $\widetilde{C}_l$ are constants, given by

$$C_j = e^{2\left(\pi\sigma_j^2+\mu_j\right)}, \forall j \in \{r, s, z\} \quad (39)$$

$$\widetilde{C}_l = e^{\frac{\pi\sigma_l^2}{2}+\mu_l}, \forall l \in \{r, Z_1, Z_1\} \quad (40)$$

σ_η^2 is the total noise power in the state η, and p_η is the occurrence probability of the state η.

Proof: See Appendix B.

Based on (35), we can obtain the closed-form expression for SER of the PLC OFDM system as

$$P_{\text{SER}} = 1 - \left(1 - 2\left(1-\frac{1}{\sqrt{\theta}}\right) Q\left(\sqrt{\frac{3\gamma}{\theta-1}}\right)\right)^2 \quad (41)$$

where θ is the constellation order, and γ is the output SNR.

V. SIMULATION RESULTS

In this section, we present numerical results. We use MATLAB to build Monte Carlo simulations for the PLC-MIMO system, as shown in Fig. 2. The 16-QAM is adopted to modulate input signals for the OFDM system. The simulation results are used to compare with those found from the developed analytical model. The simulation parameters are chosen based on the HomePlug AV2 standard [35], configured as Table I.

Fig. 5 shows the sum data rate curves of receiving ports against the noise in various noise states. It can be noticed that

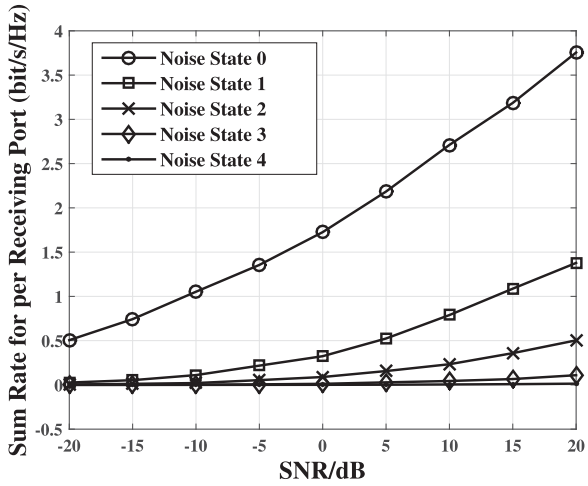

Fig. 5. Comparison of the sum data rate of receiving ports against the SNR among five noise states.

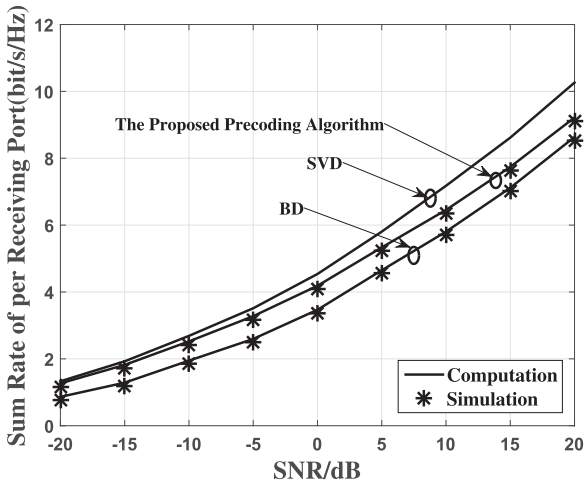

Fig. 6. Comparison of the sum data rate of receiving ports against the SNR among three precoding algorithms.

the dominant of the sum data rate are those achieved when the system is in state 0 and state 1. The sum data rate becomes smaller with the increasing of the state number. Especially, when the system is in the state whose state number is larger than four, the sum data rate is around zero. The reason is with the increasing of the state number, the occurrence probability of the corresponding state decreases dramatically. As a result, the sum data rate in these states whose number is larger than five is very small.

Fig. 6 demonstrates curves of the sum data rate achieved by different precoding algorithms. The numerical curves are obtained by using the closed-form expression given by (25). It follows from the figure that the analytical results and the simulation results are consistent. The result also shows that the sum data rate of the proposed precoding algorithm is better than that of the block diagonalization (BD) and corresponds closely to that of SVD in the case of low SNR ratio. With the increase of SNR, the performance of the proposed precoding algorithm is worse than that of SVD, but still much better than that of BD.

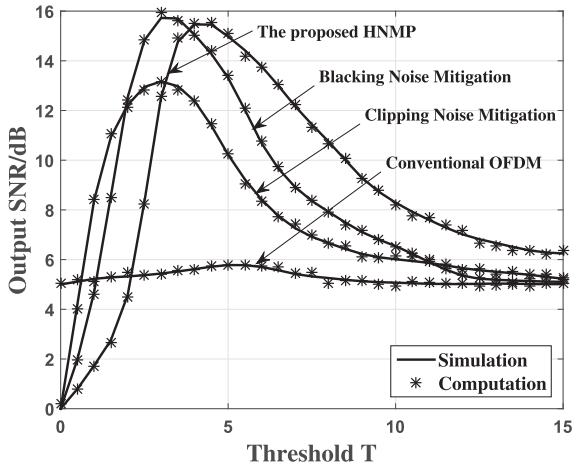

Fig. 7. Comparison of the output SNR when adopting different thresholds among different noise mitigation methods and the PLC-OFDM system without adopting noise mitigation.

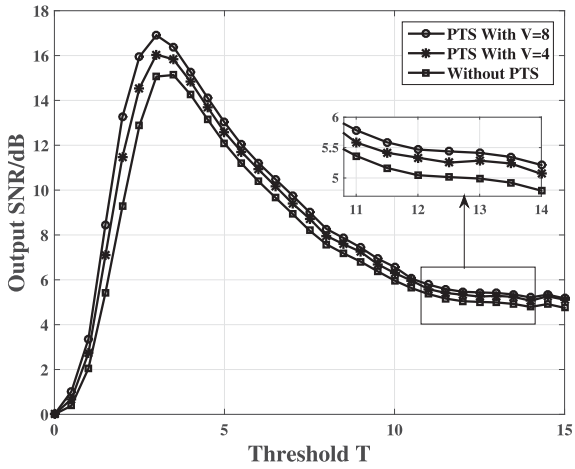

Fig. 8. Comparison of output SNR against thresholds among HNMP without adopting PTS, HNMP adopting PTS with $K = 4$, and HNMP adopting PTS with $K = 8$. K is the number of sub-carriers of the OFDM system.

Therefore, the proposed precoding approach can improve the performance of practical PLC systems.

To evaluate the performance of the proposed hybrid noise mitigation method, we need to select an appropriate threshold T for (32). However, it is very difficult to derive the optimal value for the threshold in theory. Thus, we use the experimental way to specify the threshold. As shown in Fig. 7, if the threshold is set as two or three, the PLC system can achieve the best output SNR as using clipping noise mitigation. We also notice that when the threshold is set as four for blanking noise mitigation, the receiver can obtain the best SNR. Consequently, we choose three as the threshold for the clipping noise mitigation and four as the threshold for the blanking one. However, if the threshold T is larger than six, the output SNR decreases dramatically. The reason is that the threshold is used to mitigate noise signals whose amplification is large than the threshold. When T is larger than six, the noise mitigation algorithms cannot work effectively to mitigate the noise with power lower than six. In addition, we observe that the numerical results, obtained with (35), are almost consistent with the simulation ones, with a small performance gap.

Fig. 8 indicates the figure of output SNR for the HNMP against the threshold. We observe that the noise mitigation can improve the performance on SNR by introducing PTS to the noise mitigation system. Furthermore, as we select the appropriate threshold, such as $T = 4$, the output SNR in HNMP based on PTS is much better than that without PTS.

Fig. 9 evidences the SER curves obtained by (41) against signal to impulsive noise ratio (SIPNR). In this simulation, the HNMP is designed based on PTS with $K = 8$, where K is the number of sub-carriers of the OFDM system. It can be seen from the figure that the analytical results and the simulation results are consistent. Also, we notice that the noise mitigation can significantly improve the SER performance, when compared to the PLC-OFDM system without noise mitigation. Since the power ratio of signal to impulsive noise reduces with the increasing power of impulsive noise, SER of the system without adopting noise mitigation increases dramatically. However, SER of

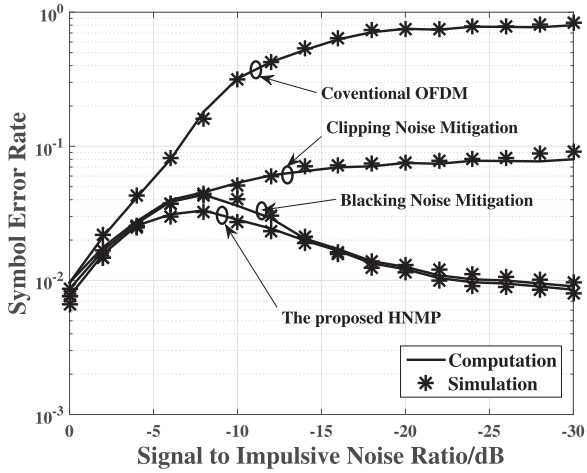

Fig. 9. SER at the output of 16-QAM OFDM demodulator against signal to impulsive noise ratio. The threshold T is set as three and four for clipping and blanking noise algorithms, respectively.

systems adopting HNMP and blanking noise mitigation decreases due to removing of the impulsive noise signal. Nonetheless, if the SIPNR is between -10 dB and -5 dB, the impulsive noise is very difficult to be removed by mitigation algorithms, which leads to SER getting their large values. As SIPNR is lower than -10 dB, SER decreases fast. Furthermore, in the case of low SIPNR, SER of HNMP is almost the same with and slightly better than that of blanking noise mitigation.

VI. Conclusion

In this paper, we design a PLC-MIMO system to improve the data rate, where multiple wires are used as communication channels subject to the impulsive and the Gaussian noises. Then, we develop a precoding scheme by maximizing the sum data rate. In consorting to this, we further derive a closed-form of the sum data rate for the PLC-MIMO system in each Markov state. In order to improve the system performance, we adopt a hybrid noise mitigation scheme to reduce channel noises. We use PTS

to reduce the PAPR of transmitting signals for protecting the useful signal from being mitigated. A hybrid approach of the blanking and clipping noise mitigation is used to mitigate the channel noise. Finally, the closed-form for the output SNR of the HNMP is derived. Simulation results reveal that our precoding scheme achieves a better sum data rate as compared to the traditional precoding schemes, and the proposed HNMP can considerably improve the SER performance.

APPENDIX A
PROOF OF THEOREM 1

Proof: The achievable data rate of the nth receiving port in the ηth state can be expressed as the mutual information of s_n and y_n, given as

$$I^{(\eta)}\left(x_n, y_n\right) = \log_2\left(1 + \widehat{\mathbf{h}}_n \mathbf{w}_n^{(\eta)} {\mathbf{w}_n^{(\eta)}}^H \widehat{\mathbf{h}}_n^H \times \left({\sigma_n^{(\eta)}}^2 + \widehat{\mathbf{h}}_n \sum_{t=1, j\neq n}^{N} \mathbf{w}_t^{(\eta)} {\mathbf{w}_t^{(\eta)}}^H \widehat{\mathbf{h}}_t^H\right)^{-1}\right). \tag{42}$$

We then prove the problem in two cases. In the first case, we derive the data rate of the nth receiving port, which can be expressed as

$$\begin{aligned} I\left(x_n, {y_n}^{(\eta)}\right) &= R_{\text{sum}}^{(\eta)}(n) \\ &= \log_2 \times \left(1 + \frac{{\mathbf{w}_n^{(\eta)}}^H \widehat{\mathbf{h}}_n^H \widehat{\mathbf{h}}_n \mathbf{w}_n^{(\eta)}}{{\sigma_n^{(\eta)}}^2 + \sum_{t=1, t\neq n}^{N} {\mathbf{w}_t^{(\eta)}}^H \widehat{\mathbf{h}}_n^H \widehat{\mathbf{h}}_n \mathbf{w}_t^{(\eta)}}\right) \\ &= \log_2\left(\frac{{\mathbf{w}_n^{(\eta)}}^H \mathbf{B}_{n,n}^{(\eta)} \mathbf{w}_n^{(\eta)}}{{\mathbf{w}_n^{(\eta)}}^H \mathbf{A}_{n,n}^{(\eta)} \mathbf{w}_n^{(\eta)}}\right). \end{aligned} \tag{43}$$

In the second case, we calculate the sum data rate of the other receiving $N-1$ ports, given as

$$I^{(\eta)}\left(s_t, y_t\right) = \log_2\left(1 + \widehat{\mathbf{h}}_t \mathbf{w}_t^{(\eta)} {\mathbf{w}_t^{(\eta)}}^H \widehat{\mathbf{h}}_t^H \times \left(r_t + \widehat{\mathbf{h}}_t \mathbf{w}_n^{(\eta)} {\mathbf{w}_n^{(\eta)}}^H \widehat{\mathbf{h}}_t^H\right)^{-1}\right) \tag{44}$$

where r_t can be expressed as

$$r_t = {\sigma_n^{(\eta)}}^2 + \widehat{\mathbf{h}}_n \sum_{t=1, j\neq n}^{N} \mathbf{w}_t^{(\eta)} {\mathbf{w}_t^{(\eta)}}^H \widehat{\mathbf{h}}_t^H. \tag{45}$$

Hence, the sum data rate of the N ports can be obtained as

$$R_{\text{sum}}^{(\eta)}(t) = \sum_{t=1, j\neq n}^{N} \log_2\left(\frac{{\mathbf{w}_n^{(\eta)}}^H \mathbf{B}_{t,n}^{(\eta)} \mathbf{w}_n^{(\eta)}}{{\mathbf{w}_n^{(\eta)}}^H \mathbf{A}_{t,n}^{(\eta)} \mathbf{w}_n^{(\eta)}}\right). \tag{46}$$

By combining (43) and (46), (20) holds. This completes Theorem 1. ■

APPENDIX B
PROOF OF THEOREM 2

Proof: According to (33) and (34), the receiving SNR can be expressed as

$$\gamma = \frac{\mathbb{E}\left(\left|\mathcal{K} \cdot h_{n,m} x_n\right|^2\right)}{\mathbb{E}\left(\left|y_n - \mathcal{K} h_{n,m} x_n\right|^2\right)} = \left(\frac{\mathbb{E}\left(\left|y_n\right|^2\right)}{2h_{m,n}^2 \mathcal{K}^2} - 1\right)^{-1}. \tag{47}$$

Let $P_{\text{out}} = \mathbb{E}(|y_n|^2)$, (35) directly holds.

We then derive the closed-form for P_{out} and $\mathcal{K}$. After passing through noise mitigation processor, the power of the output signal is given as

$$\begin{aligned} P_{\text{out}} = &\sum_{\eta=1}^{\Theta} \mathbb{E}\left(|y_n|^2 | D_0, \eta\right) \Pr(D_0, \eta) \\ &+ \sum_{\eta=1}^{\Theta} \mathbb{E}\left(|y_n|^2 | D_1, \eta\right) \Pr(D_1, \eta) \end{aligned} \tag{48}$$

where $\Pr(D_0, \eta)$ is probability that the event D_0 occurrence in the η state.

According to the work presented in [10], the fading amplitude of the PLC channel is a log-normal distribution. Then, we express the PDF $f\left(|y_n| \, | D_0, \eta\right)$ by defining $A_r = |y_n|$, given as

$$f\left(A_r \, | D_0, \eta\right) = \begin{cases} \frac{p_\eta}{A_r \sqrt{2\pi\sigma_\eta^2}} e^{-\frac{(\ln A_r - \mu_r)^2}{2\pi\sigma_\eta^2}}, & 0 \leq A_r \leq T \\ 0, & \text{otherwise.} \end{cases} \tag{49}$$

Then, $\Pr(D_0, \eta)$ can be given as

$$\begin{aligned} \Pr(D_0, \eta) &= \int_0^T \frac{p_\eta}{A_r \sqrt{2\pi\sigma_\eta^2}} e^{-\frac{(\ln A_r - \mu_r)^2}{2\pi\sigma_\eta^2}} dA_r \\ &= p_\eta \int_{-\infty}^{\frac{\ln T - \mu_r}{\sqrt{2\pi\sigma_\eta^2}}} e^{-x^2} dx. \end{aligned} \tag{50}$$

With (38) and (40), (50) can be simplified as

$$\Pr(D_0, \eta) = p_\eta Q_r(T). \tag{51}$$

Similarly, $\mathbb{E}(|y_n|^2 | D_0, \eta)$ in (48) can be expressed as

$$\begin{aligned} \mathbb{E}\left(|y_n|^2 | D_0, \eta\right) &= \int_0^T A_r^2 \frac{p_\eta}{A_r \sqrt{2\pi\sigma_\eta^2}} e^{-\frac{(\ln A_r - \mu_r)^2}{2\pi\sigma_\eta^2}} dA_r \\ &= p_\eta e^{2\left(\pi\sigma_\eta^2 + \mu_r\right)} \int_{-\infty}^{\frac{\ln T - \mu_r}{\sqrt{2\pi\sigma_\eta^2}}} e^{-\left(t - \sqrt{2\pi\sigma_\eta^2}\right)^2} dt \\ &= p_\eta C_r \int_{-\infty}^{\frac{\ln\left(T e^{-2\pi\sigma_\eta^2}\right) - \mu_r}{\sqrt{2\pi\sigma_\eta^2}}} e^{-x^2} dx. \end{aligned} \tag{52}$$

Also, (52) can be simplified as

$$\mathbb{E}\left(|y_n|^2 \, | D_0, \eta\right) = p_\eta C_r Q_r\left(T e^{-2\pi\sigma_\eta^2}\right). \tag{53}$$

With the same method, we have

$$\Pr(D_1,\eta) = p_\eta \left(Q_r\left(aT\right) - Q_r(T)\right). \tag{54}$$

Then, we obtain

$$\mathbb{E}\left(|y_n|^2|D_1,\eta\right) = p_\eta C_r\left(Q_r\left(aTe^{-2\pi\sigma_\eta^2}\right) - Q_r\left(Te^{-2\pi\sigma_\eta^2}\right)\right). \tag{55}$$

Substituting (51) and (55) into (48), (36) holds.

Similarly, we can express $\mathcal{K}$ as

$$\mathcal{K} = \frac{1}{2}\sum_{\eta=1}^{\Theta}\mathbb{E}\left(y_n x_n^*|D_0,\eta\right)\Pr(D_0,\eta) + \frac{1}{2}\sum_{\eta=1}^{\Theta}\mathbb{E}\left(Te^{j\arg(x_n+z_n)}x_n^*|D_1,\eta\right)\Pr(D_1,\eta). \tag{56}$$

The first item of (56) can be expressed by the similar approach to cope with (48). Then, we have

$$\mathbb{E}\left(y_n x_n^*|D_0,\eta\right) = \frac{1}{2}\mathbb{E}\left(|y_n|^2|D_0,\eta\right) - \frac{1}{2}\mathbb{E}\left(|x_n|^2|D_0,\eta\right) - \frac{1}{2}\mathbb{E}\left(|z_n|^2|D_0,\eta\right). \tag{57}$$

For simplicity, we define $A_x = |x_n|$ and $A_z = |z_n|$. To derive $\mathbb{E}(|x_n|^2 \mid D_0,\eta)$, we express the PDF of $(|x_n| \mid D_0,\eta)$ as

$$f\left(A_x \mid D_0,\eta\right) = \frac{f\left(A_x\right)\Pr\left(D_0|A_x,\eta\right)}{\Pr\left(D_0|\eta\right)}. \tag{58}$$

Suppose that A_x follows the log-normal distribution with the parameter (u_s,σ_s^2) and A_z follows the normal distribution with the parameters (u_z,σ_z^2). Furthermore, A_x and A_z are independent. Then, we derive the PDF of $A_x + A_z$ as

$$\begin{aligned} f_{A_x+A_z}(w) &= \int_0^\infty f_z(A_z) f_s(w-A_z) dA_z \\ &= \int_0^\infty \frac{1}{(w-A_z)2\pi\sigma_s^2\sigma_z^2} \\ &\quad \times e^{-\left(\frac{(\ln(w-A_z)-\mu_s)^2}{2\pi\sigma_s^2} + \frac{(A_z-\mu_z)^2}{2\pi\sigma_z^2}\right)} dA_z \end{aligned} \tag{59}$$

where w denotes $A_x + A_z$, and f_z and f_s are the PDF of A_z and A_x.

According to the work presented in [12], we have the approximation

$$\int_0^\infty f(x)\cdot e^{-x^2}dx \approx \sum_{i=1}^{N} H_i \cdot f(x). \tag{60}$$

Therefore, (59) can be approximated as

$$f_{A_x+A_z}(w) = \sum_{i=1}^{N} H_i \cdot \frac{1}{(w-\xi_i)\sqrt{2\pi\sigma_s^2}} e^{-\frac{\left(\ln(w-\xi_i)-\mu_s\right)^2}{2\pi\sigma_s^2}}. \tag{61}$$

Then, we have

$$\begin{aligned} \Pr\left(D_0|A_x,\eta\right) &= \int_0^{T-\sigma_{g_\eta}^2} f_{A_x+A_z}(w)\,dw \\ &= \int_0^{T-\sigma_{g_\eta}^2} \sum_{i=1}^{N} H_i \\ &\quad \cdot \frac{1}{(w-\xi_i)\sqrt{2\pi\sigma_s^2}} e^{-\frac{\left(\ln(w-\xi_i)-\mu_s\right)^2}{2\pi\sigma_s^2}} dw \\ &= \sum_{i=1}^{N} H_i \int_{-\infty}^{\frac{\ln\left(T-\sigma_{g_\eta}^2-\xi_i\right)-\mu_s}{\sqrt{2\pi\sigma_s^2}}} e^{-x^2}dx. \end{aligned} \tag{62}$$

As in (51), we simplify (62) as

$$\Pr\left(D_0|A_x,\eta\right) = \sum_{i=1}^{N} H_i \cdot Q_s\left(T - \sigma_{g_\eta}^2 - \xi_i\right). \tag{63}$$

Thus, $f(A_s|D_0,\eta)$ in (58) is obtained as

$$f\left(A_x|D_0,\eta\right) = \frac{\sum_{i=1}^{N} H_i \cdot Q_s\left(T-\sigma_{g_\eta}^2-\xi_i\right)}{p_\eta Q_r(T)} f(A_x). \tag{64}$$

Plug (63) into (52), $\mathbb{E}(|s_k|^2|D_0,\eta)$ is

$$\mathbb{E}\left(|x_n|^2|D_0,\eta\right) = \frac{\sum_{i=1}^{N} H_i \cdot Q_s\left(T-\sigma_{g_\eta}^2-\xi_i\right)}{p_\eta Q_r(T)} \times C_s Q_s\left(Te^{-2\pi\sigma_s^2}\right). \tag{65}$$

By using the same method with (65), we have

$$\mathbb{E}\left(|z_n|^2|D_0,\eta\right) = \frac{\sum_{i=1}^{N} H_i \cdot Q_z\left(T-\sigma_{g_\eta}^2-\xi_i\right)}{p_\eta Q_r(T)} \times C_z Q_z\left(Te^{-2\pi\sigma_z^2}\right). \tag{66}$$

In addition, the second item of the right hand in (56) can be expressed as the work presented in [18]

$$\mathbb{E}\left(Te^{j\arg(x_n(f)+z_n(f))}s_b^*|D_1,\eta\right) = \frac{T}{2}\left(\mathbb{E}\left(|\tilde{v}_k||D_1,\eta\right) + \mathbb{E}\left(|Z_1||D_1,\eta\right) + \mathbb{E}\left(|Z_2||D_1,\eta\right)\right) \tag{67}$$

where Z_1 and Z_2 are the random variables defined as $Z_1 = A_x^2/A_r$ and $Z_2 = A_z^2/A_r$.

With the integral method given in (55), we can obtain

$$\mathbb{E}\left(|\tilde{v}_k||D_1,\eta\right) = p_\eta \widetilde{C}_r\left(Q_r\left(aTe^{-\pi\sigma_\eta^2}\right) - Q_r\left(Te^{-\pi\sigma_\eta^2}\right)\right). \tag{68}$$

We define $Z_1 = A_x^2/A_r$ and thus Z_1 follows the log-normal distribution with parameter $(2\mu_s - \mu_r, 4\sigma_s^2 + \sigma_\eta^2)$. For simplicity, we define $\mu_{Z_1} = 2\mu_s - \mu_r$ and $\sigma_{Z_1}^2 = 4\sigma_s^2 + \sigma_\eta^2$. In this

case, it follows that

$$\mathbb{E}\left(|Z_1||D_1,\eta\right) = p_\eta \widetilde{C}_{Z_1}\left(Q_{Z_1}\left(aTe^{-\pi\sigma_{Z_1}^2}\right) - Q_{Z_1}\left(Te^{-\pi\sigma_{Z_1}^2}\right)\right). \quad (69)$$

Similarly, we have

$$\mathbb{E}\left(|Z_2||D_1,\eta\right) = p_\eta \widetilde{C}_{Z_2}\left(Q_{Z_2}\left(aTe^{-\pi\sigma_{Z_2}^2}\right) - Q_{Z_2}\left(Te^{-\pi\sigma_{Z_2}^2}\right)\right). \quad (70)$$

Combining (53), (55), (56), (65), and (66), we can obtain (37). This completes Theorem 2. ■

REFERENCES

[1] Y. Qian, M. Tian, X. Jian, F. Shu, and J. Li, "Performance analysis for a two-way relaying power line network with analog network coding," *Frontiers Inf. Technol. Electron. Eng.*, vol. 16, no. 10, pp. 892–898, 2015.

[2] T. Sung and A. Bojanczyk, "Optimal power control and relay capacity for PLC-embedded cooperative systems," in *Proc. 7th IEEE Conf. Consum. Commun. Netw. Conf.*, NJ, USA, 2010, pp. 813–817.

[3] L. T. Berger, A. Schwager, P. Pagani, and D. M. Schneider, "MIMO power line communications," *IEEE Commun. Surv. Tut.*, vol. 17, no. 1, pp. 106–124, Jan.–Mar. 2014.

[4] K. Khalil, M. G. Gazalet, P. Corlay, and F. X. Coudoux, "An MIMO random channel generator for indoor power-line communication," *IEEE Trans. Power Del.*, vol. 29, no. 4, pp. 1561–1568, Aug. 2014.

[5] J. Peng, "Linear precoding design for MIMO-PLC systems," *Tsinghua Sci. Technol.*, vol. 20, no. 2, pp. 155–163, 2015.

[6] C. Xiao, Y. R. Zheng, and Z. Ding, "Globally optimal linear precoders for finite alphabet signals over complex vector gaussian channels," *IEEE Trans. Signal Process*, vol. 59, no. 7, pp. 3301–3314, Jul. 2011.

[7] M. Wang, W. Zeng, C. Xiao, and W. Zeng, "Practical linear precoder design for finite alphabet multiple-input multiple-output orthogonal frequency division multiplexing with experiment validation," *IET Commun.*, vol. 7, no. 8, pp. 836–847, 2013.

[8] M. Sayed, I. H. Kim, T. Pande, and A. Batra, "Proposed frame and preamble structure for MIMO narrowband power line communications," in *Proc. IEEE Int. Symp. Power Line Commun. Appl.*, Austin, TX, USA, 2015, pp. 65–70.

[9] S. Galli, A. Scaglione, and Z. Wang, "For the grid and through the grid: The role of power line communications in the smart grid," *Proc. IEEE*, vol. 99, no. 6, pp. 998–1027, Jun. 2011.

[10] A. Dubey, R. K. Mallik, and R. Schober, "Performance analysis of a power line communication system employing selection combining in correlated lognormal channels and impulsive noise communications," *IET Commun.*, vol. 8, no. 7, pp. 1072–1082, 2014.

[11] A. Nayagam, S. Katar, D. Rende, K. Afkhamie, and L. Yonge, "Tradeoff between channel estimation accuracy and application throughput for in-home MIMO power line communication," in *Proc. IEEE Int. Symp. Power Line Commun. Appl.*, Udine, 2011, pp. 411–417.

[12] D. Schneider, J. Speidel, L. Stadelmeier, and D. Schill, "Precoded spatial multiplexing MIMO for inhome power line communications," in *Proc. Global Telecommun. Conf.*, New Orleans, LO, USA, 2008, pp. 1–5.

[13] M. Biagi and V. Polli, "Iterative multiuser resource allocation for inhome power line communications," in *Proc. IEEE Int. Symp. Power Line Commun. Appl.*, Udine, 2011, pp. 388–392.

[14] A. Chaudhuri and M. R. Bhatnagar, "Optimised resource allocation under impulsive noise in power line communications," *IET Commun.*, vol. 8, no. 7, pp. 1104–1108, 2013.

[15] T. N. Vo, K. Amis, T. Chonavel, and P. Siohan, "Influence of interference in MIMO power line communication systems," in *Proc. IEEE Int. Symp. Power Line Commun. Appl.*, Glasgow, 2014, pp. 255–260.

[16] M. J. Rahman and L. Lampe, "Interference alignment for MIMO power line communications," in *Proc. Power Line Commun. Appl.*, Austin, TX, USA, 2015, pp. 71–76.

[17] S. V. Zhidkov, "Performance analysis and optimization of OFDM receiver with blanking nonlinearity in impulsive noise environment," *IEEE Trans. Veh. Technol.*, vol. 55, no. 1, pp. 234–242, Jan. 2006.

[18] V. Zhidkov, "Analysis and comparison of several simple impulsive noise mitigation schemes for OFDM receivers," *IEEE Trans. Commun.*, vol. 56, no. 1, pp. 5–9, Jan. 2008.

[19] E. Alsusa and K. Rabie, "Dynamic peak-based threshold estimation method for mitigating impulsive noise in power-line communication system," *IEEE Trans. Power Del.*, vol. 28, no. 4, pp. 2201–2208, Oct. 2013.

[20] K. Rabie and E. Alsusa, "Quantized peak based impulsive noise blanking in power-line communications," *IEEE Trans. Power Del.*, vol. 29, no. 4, pp. 1630–1638, Aug. 2014.

[21] S. H. Muller and J. B. Huber, "OFDM with reduced peak-to-average power ratio by optimum combination of partial transmit sequences," *Electron. Lett.*, vol. 33, no. 5, pp. 1368–369, 1997.

[22] K. Rabie and E. Alsusa, "On enhancing the performance of the DPTE-based noise cancellation method utilizing the PTS PAPR reduction scheme in PLC systems," in *Proc. 18th IEEE Int. Symp. Power Line Commun. Appl.*, Beijing, 2015, pp. 1–6.

[23] K. Rabie and E. Alsusa, "Improved DPTE technique for impulsive noise mitigation over power-line communication channels," *Int. J. Electron. Commun.*, vol. 69, pp. 1847–1853, 2015.

[24] B. Adebisi, K. Rabie, A. Ikpehai, C. Soltanpur, and A. Wells, "Vector OFDM transmission over non-Gaussian power line communication channels," *IEEE Syst. J.*, vol. 12, no. 3, pp. 2344–2352, Sep. 2018.

[25] Y. Zhuang and L. Lampe, "Physical layer security in MIMO power line communication networks," in *Proc. IEEE Int. Symp. Power Line Commun. Appl.*, Glasgow, 2014, pp. 272–277.

[26] M. Zimmermann and K. Dostert, "A multipath model for the powerline channel," *IEEE Trans. Commun.*, vol. 50, no. 4, pp. 553–559, Apr. 2002.

[27] B. Nikfar, T. Akbudak, and A. J. H. Vinck, "MIMO capacity of class a impulsive noise channel for different levels of information availability at transmitter," in *Proc. IEEE Int. Symp. Power Line Commun. Appl.*, Glasgow, 2014, pp. 266–271.

[28] Y. H. Ma, P. L. So, and E. Gunawan, "Performance analysis of OFDM systems for broadband power line communications under impulsive noise and multipath effects," *IEEE Trans. Power Del.*, vol. 20, no. 2, pp. 674–682, Apr. 2005.

[29] K. C. Wiklundh, P. F. Stenumgaard, and H. M. Tullberg, "Channel capacity of middletons class a interference channel," *Electron. Lett.*, vol. 45, no. 24, pp. 1227–1229, 2009.

[30] N. Lee, H. Yang, and J. Chun, "Achievable sum-rate maximizing AF relay beamforming scheme in two-way relay channels," in *Proc. IEEE Int. Conf. Commun. Workshops*, Beijing, 2008, pp. 300–305.

[31] F. J. C. Corripio, J. A. C. Arrabal, L. D. del Rio, and J. T. E. Munoz, "Analysis of the cyclic short-term variation of indoor power line channels," *IEEE J. Sel. Areas Commun.*, vol. 24, no. 7, pp. 1327–1338, Jul. 2006.

[32] D. V. Chi, "Performance analysis and enhancement of OFDM-based WLAN Systems in the presence of nonlinear HPAS and narrowband interference for single and multiple transmit antennas" Ph.D. dissertation, Dept. Elect. Eng., Univ. California, San Diego, CA, USA, 2012.

[33] K. M. Rabie and E. Alsusa, "Improving blanking/clipping based impulsive noise mitigation over powerline channels," in *Proc. Pers. Indoor Mobile Radio Commun.*, London, 2013, pp. 3413–3417.

[34] P. Banelli, "Theoretical analysis and performance of OFDM signals in nonlinear fading channels," *IEEE Trans. Wireless Commun.*, vol. 2, no. 2, pp. 284–293, Mar. 2003.

[35] H. P. Alliance, "Homeplug AV white paper," HomePlug Powerline Alliance Inc., Tech. Rep. HPAVWP-050818, 2005. [Online]. Available: http://www.homeplug.org/media/filer_public/b8/68/b86828d9-7e8a-486f-aa82-179e6e95cab5/hpav-white-paper_050818.pdf

Yuwen Qian received the Ph.D. degree in automatic engineering from the Nanjing University of Science and Technology, Nanjing, China, in 2011.

From July 2002 to June 2011, he was a Lecturer with the School of Automation, Nanjing University of Science and Technology. Since October 2011, he has been a Lecturer with the School of Electronic and Optical Engineering, Nanjing University of Science and Technology. His main research interests are information security, smart grid, and power line communications.

Xiangwei Zhou received the B.S. degree in communication engineering from the Nanjing University of Science and Technology, Nanjing, China, the M.S. degree in information and communication engineering from Zhejiang University, Hangzhou, China, and the Ph.D. degree in electrical and computer engineering from the Georgia Institute of Technology, Atlanta, GA, USA, in 2005, 2007, and 2011, respectively.

Since August 2015, he has been an Assistant Professor with the Division of Electrical and Computer Engineering, Louisiana State University, Baton Rouge, LA, USA. From 2013 to 2015, he was an Assistant Professor with the Department of Electrical and Computer Engineering, Southern Illinois University, Carbondale, IL, USA, and from 2011 to 2013, a Senior Systems Engineer with Marvell Semiconductor, Santa Clara, CA, USA. His research interests include wireless communications, statistical signal processing, and cross-layer optimization, with current emphasis on spectrum-efficient, energy-efficient, and secure communications, coexistence of wireless systems, and machine learning for intelligent communications.

Dr. Zhou was the recipient of the Best Paper Award at the 2014 International Conference on Wireless Communications and Signal Processing.

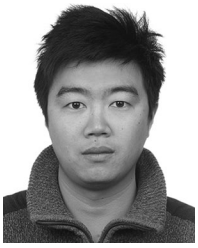

Jun Li received the Ph.D. degree in electronic engineering from Shanghai Jiao Tong University, Shanghai, China in 2009.

From January 2009 to June 2009, he was a Research Scientist with the Department of Research and Innovation, Alcatel Lucent Shanghai Bell. From June 2009 to April 2012, he was a Postdoctoral Fellow with the School of Electrical Engineering and Telecommunications, University of New South Wales, Australia. From April 2012 to June 2015, he was a Research Fellow with the School of Electrical Engineering, University of Sydney, Australia. Since June 2015, he is a Professor with the School of Electronic and Optical Engineering, Nanjing University of Science and Technology, Nanjing, China. His research interests include network information theory, channel coding theory, wireless network coding, and resource allocations in cellular networks.

Feng Shu received the B.S. degree from XiDian University, Xian, China, in 1997, the M.S. degree from Fuyang Teaching College, Fuyang, China, in 1994, and the Ph.D. degree from Southeast University, Nanjing, China, in 2002.

From October 2003 to October 2005, he was a Postdoctoral Researcher with the National Key Mobile Communication Lab, Southeast University. From September 2009 to September 2010, he was a Visiting Postdoctor with the University of Texas at Dallas. In October 2005, he joined the School of Electronic and Optical Engineering, Nanjing University of Science and Technology, Nanjing, China, where he is currently a Professor and Supervisor of Ph.D. and graduate students. His research interests include wireless networks, wireless location, and array signal processing.

Dushantha Nalin K. Jayakody (M'14) received the B.Eng. degree (with first-class hons.) from Dawood University of Engg. & Tech., Pakistan in 2009 and was ranked as the merit position holder of the university (under SAARC Scholarship). He received the M.Sc. degree in electronics and communications engineering from the Department of Electrical and Electronics Engineering, Eastern Mediterranean University, Famagusta, Cyprus, in 2010 (under the University Full Graduate Scholarship) and ranked as the first merit position holder of the department. He received the Ph.D. degree in electronics and communications engineering in 2014, from University College Dublin, Dublin, Ireland.

From September 2014 to September 2016, he held a Postdoctoral position with the Coding and Information Transmission Group, University of Tartu, Tartu, Estonia, and the University of Bergen, Bergen, Norway. Since 2016, he has been a Professor with the Department of Control System Optimization, Institute of Cybernetics, National Research Tomsk Polytechnic University, Tomsk, Russia.

Dr. Jayakody was the Session Chair or Technical Program Committee Member for various international conferences, such as IEEE PIMRC 2013/2014, IEEE WCNC 2014/2016, IEEE VTC 2015, etc.